Investigating interaction-induced chaos using time-dependent density-functional theory

Adam Wasserman,[1] Neepa T. Maitra,[2] and Eric J. Heller[1,3]
[1]*Department of Chemistry and Chemical Biology, Harvard University, 12 Oxford Street, Cambridge, Massachusetts 02138, USA*
[2]*Department of Physics and Astronomy, Hunter College and City University of New York, 695 Park Avenue, New York, New York 10021, USA*
[3]*Department of Physics, Harvard University, 17 Oxford Street Cambridge, Massachusetts 02138, USA*
(Received 26 January 2007; published 1 April 2008)

Systems whose underlying classical dynamics are chaotic exhibit signatures of the chaos in their quantum mechanics. We investigate the possibility of using the linear response formalism of time-dependent density functional theory (TDDFT) to study the case when chaos is induced by electron-interaction alone. Nearest-neighbor level-spacing statistics are in principle exactly and directly accessible from TDDFT. We discuss how the TDDFT linear response procedure can reveal information about the mechanism of chaos induced by electron-interaction alone. A simple model of a two-electron quantum dot highlights the necessity to go beyond the adiabatic approximation in TDDFT.

DOI: 10.1103/PhysRevA.77.042503 PACS number(s): 31.15.E−, 31.10.+z, 05.45.Mt, 73.21.La

I. INTRODUCTION

The study of the quantum mechanics of systems whose underlying classical dynamics are chaotic, has revealed many intriguing features. It is now well established that underlying classical chaos dramatically manifests itself in certain quantum signatures: spectral fluctuations, localization properties of wave functions, inverse participation ratios, and extreme sensitivity to tiny variations in control parameters [1]. Perhaps the most widely studied of these is the spectral statistics: In particular, the nearest-neighbor spacing distributions (NNS) for integrable systems generically display Poissonian statistics (level clustering), while displaying Wigner-Dyson statistics (level repulsion) for chaotic systems. Such correspondence between classical chaos and NNS statistics was conjectured by Bohigas, Giannoni, and Schmit [2], and while counterexamples exist [3,4], the association is so general that Wigner-Dyson statistics are often viewed as signatures of underlying classical chaos. This property has been used to study the transition from integrability to chaos as a parameter in the confining potential of the system is varied [5]. Many of these studies consider one particle, or, in quantum dots, noninteracting electrons; the chaos arises in such cases due to the shape of the dot confining potential. What is less well understood is what happens when electron-interaction is turned on. Suppose that interacting electrons are placed in a potential where the single-particle NNS is Poissonian; is the chaos induced by the Coulomb interaction enough to transform the NNS statistics to a Wigner-Dyson distribution? To what extent does the level repulsion kick in? Is the picture qualitatively different with few electrons compared to many electrons?

That electron-interaction alone can induce chaos is certainly evident from the very early days of quantum mechanics, impeding Bohr in 1913 from successfully quantizing the helium atom [6] (task only completed semiclassically in 1991 [7]; for a beautiful review of the theory of two-electron atoms, see Ref [8].). Putting aside concerns regarding the validity of random-matrix theory when two-body interactions are present [9], we note that the first application of random-matrix theory outside of nuclear physics was to a series of complex atoms [10,11], where the spin-orbit interaction provided the crucial ingredient in yielding Wigner-Dyson statistics. Statistics of a different series of complex atoms based on experimental data [12], as well as theoretical models [13] support the finding that highly excited states of complex atoms tend to display Wigner-Dyson statistics. There have been several studies in molecules (e.g., Ref. [14]) where the coupling of electronic excitations with nuclear vibrational and rotational excitations provide the complexity. Generally, experimental data, with many levels of the same symmetry, is needed. The chaos in these examples is understood to arise not from Coulomb electron-interaction alone but rather from its coupling to other degrees of freedom.

For simple atoms, there have been very few calculations of the level-spacing statistics, perhaps because of the challenges involved in gathering enough levels of doubly excited resonances, either from theory or experiment, which appear to be crucial for this effect (see Ref. [15] for a calculation of level-repulsion in helium). However deviations from Poissonian statistics have been clearly identified in nonhydrogenic Rydberg atoms in either magnetic or electric fields [16–19]. The hydrogen atom at the corresponding parameter regime is integrable, but scattering off the ionic core in a nonhydrogenic Rydberg atom creates fundamentally different dynamics, with chaotic trajectories depending on the value of the quantum defect. In models of this effect, NNS have been shown to display level-repulsion, following a distribution intermediate between Poissonian and Wigner-Dyson [16].

There are also many-electron solid-state examples, where electron-interaction has shown to lead to the transition between Poissonian and Wigner-Dyson statistics [20–23], and several of these works identify the driving parameter for this transition. Difficulties with interpreting experimental data make the idea of a theoretical calculation of the level statistics attractive. At the same time, because the solution of the interacting many-electron problem grows exponentially with the number of electrons, typically a model is used for the interaction, e.g., a two-body random interaction model was used in Ref. [20]. A recent calculation of just two electrons in a quantum dot [24], explicitly demonstrates that Coulomb

electron-interaction alone can transform the Poissonian statistics of the noninteracting system into a Wigner-Dyson system. Generally in few-electron quantum dot studies of transport [25], random constant-interaction models [26] are often used; however, Ref. [24] suggests this may not be a good description of the real interacting electronic system, as constant-interaction models retain the Poissonian statistics of the integrable noninteracting system. In order to better understand the mechanisms of interaction-induced chaos, it would be desirable to use a method that captures electron correlation reliably and efficiently (given the thousands of excited states needed in the calculation), scales well with the number of electrons, and from whose procedure one can glean aspects of the mechanism that brings about the chaos.

Time-dependent density functional theory (TDDFT) is the leading candidate for such a method. This has become the method of choice for the calculation of excitations and response properties of interacting electronic systems, because of its scalability: typically the accuracy is comparable to sophisticated wave function methods such as complete active space self-consistent field (CASSCF), while implementations follow a far cheaper scaling with system size, comparable to time-dependent Hartree-Fock (TDHF). The theory in principle yields exact excitations, but approximations for exchange-correlation effects are needed in practice. Typically, excitation energies are given to within a few tenths of an eV, although there are notorious exceptions [27,28]. There has been a tremendous drive in recent years to develop and improve the currently-available functionals.

In this paper we will explore the possibilities of using the linear response formalism of TDDFT for investigating quantum chaos induced by electron-interaction alone. This is a new area for TDDFT (here, and in what follows, by the acronym "TDDFT" we are referring to its linear-response formalism, unless otherwise stated. See Refs. [29–31] for cases that go beyond linear response). The idea is to use TDDFT to study the transition from clustering to repulsion statistics in a given system as the electron interaction is turned on. For the case of chaotic quantum dots, ground-state DFT has been used within the local spin density approximation to study the statistics of ground-state spin and spacing between conductance peaks in the Coulomb blockade regime (addition spectra) [32,33], but to our knowledge, the excited-state statistics of isolated dots with fixed number of electrons have not been studied via density functional methods. We will show in Sec. II how, by monitoring the evolution of the spectral statistics at different stages of the calculation, the TDDFT linear response framework can also shed light on the mechanism of interaction-induced chaos.

A most essential question is whether the present-day functionals are good enough to perform these tasks. In Sec. III we will give an example of a case where they are not. This example highlights an important challenge that must be overcome for TDDFT to be used in these studies. Aside from fundamental interest, it is important to characterize chaotic versus integrable dynamics for applications of technological interest, such as transport across quantum dots, highly excited atoms and molecules in external fields, quantum control and manipulation in external fields, or the engineering of quantum computer hardware that maximizes the fidelity of quantum computations [34].

II. LEVEL STATISTICS FROM TIME-DEPENDENT DENSITY FUNCTIONAL THEORY

TDDFT [35] has become the method of choice to calculate a variety of response properties of molecules, clusters, and solids, in the presence or absence of external time-dependent fields [28]. The Runge-Gross theorem provides a rigorously exact foundation for the theory: this states that given the initial state of the interacting electronic system, all observables of the system can be extracted in principle from just the time-evolving density. Most applications in chemistry and solid-state physics currently fall in the linear response regime, where TDDFT yields predictions for the optical spectra, i.e., the frequency and intensity of electronic excitations in response to electric fields [36,37].

We now explain in some detail the standard computational procedure. Consider a time-independent N-electron Hamiltonian (atomic units will be used throughout)

$$\hat{H} = \hat{T} + \hat{V}_{ee} + \int d\mathbf{r}\hat{n}(\mathbf{r})v_{\text{ext}}(\mathbf{r}), \tag{1}$$

whose energy spectrum $\{E_k\}$ we want to calculate. In Eq. (1) $\hat{T}=-1/2\Sigma_i\nabla_i^2$ stands for the N-electron kinetic energy operator, $\hat{V}_{ee}=1/2\Sigma_{i,j\neq i}|\mathbf{r}_i-\mathbf{r}_j|^{-1}$ for the electron-electron repulsion ion, $v_{\text{ext}}(\mathbf{r})$ for the external potential due to the nuclei, or applied static fields, and $\hat{n}(\mathbf{r})=\Sigma_{i=1}^{N}\delta(\mathbf{r}-\hat{\mathbf{r}}_i)$ is the density operator. The first step of a linear-response TDDFT calculation involves the self-consistent solution of the ground-state Kohn-Sham (KS) equations [38]

$$\left(-\frac{1}{2}\nabla^2 + v_s[n](\mathbf{r})\right)\phi_i(\mathbf{r}) = \varepsilon_i\phi_i(\mathbf{r}). \tag{2}$$

Here $v_s[n](\mathbf{r})$ is the KS potential defined such that N noninteracting electrons in $v_s[n](\mathbf{r})$ have the same ground-state density $n(\mathbf{r})=\langle\Psi_0|\hat{n}(\mathbf{r})|\Psi_0\rangle$ as the original interacting system of ground state $|\Psi_0\rangle$. In the KS scheme, the density is obtained from the N occupied KS orbitals as $n(\mathbf{r})=\Sigma_{i\ \text{occ}}|\phi_i(\mathbf{r})|^2$. The KS potential is written as the sum of three pieces

$$v_S[n](\mathbf{r}) = v_{\text{ext}}(\mathbf{r}) + v_H[n](\mathbf{r}) + v_{\text{XC}}[n](\mathbf{r}), \tag{3}$$

where $v_H[n](\mathbf{r})=\int d^3r' n(\mathbf{r}')/|\mathbf{r}-\mathbf{r}'|$ is the Hartree potential, and $v_{\text{XC}}[n](\mathbf{r})$ the exchange-correlation potential. This is the functional derivative (with respect to the density) of the exchange-correlation energy functional $E_{\text{XC}}[n]$, evaluated at the ground-state density $v_{\text{XC}}[n](\mathbf{r})=\delta E_{\text{XC}}[n]/\delta n(\mathbf{r})|_n$. The functional $E_{\text{XC}}[n]$ is the only quantity that needs to be approximated in order to get the ground-state density and energy; it is fortunately amenable to local approximations [39] in many situations. Knowledge of $v_{\text{XC}}(\mathbf{r})$ is sufficient to calculate the ground-state energy E_0, but the excited-state energies $\{E_k\}$, $k>0$, are not accessible from this first step. The occupied orbital energies ε_i, and KS orbitals $\phi_i(\mathbf{r})$, along with the unoccupied orbital energies and orbitals, are used as basic ingredients for the second step of the calculation. The aim of this second step is to correct the unphysical KS excitations toward the correct ones. Here one solves for eigenvalues and eigenvectors of the matrix

$$\tilde{\Omega}_{qq'} = \delta_{qq'}\omega_q^2 + 4\sqrt{\omega_q\omega_{q'}}[q|f_{\mathrm{HXC}}(\omega)|q']. \quad (4)$$

The square-root of the eigenvalues correspond to the excitation frequencies $E_k - E_0$. The double index $q=(i,a)$ represents a single excitation from occupied KS orbital $\phi_i(\mathbf{r})$ to unoccupied KS orbital $\phi_a(\mathbf{r})$, ω_q is the difference between occupied and unoccupied KS orbital energies $\omega_q = \varepsilon_a - \varepsilon_i$, and

$$[q|f_{\mathrm{HXC}}(\omega)|q'] = \int d\mathbf{r}d\mathbf{r}'\,\phi_i^*(\mathbf{r})\phi_a(\mathbf{r}) \times f_{\mathrm{HXC}}(\mathbf{r},\mathbf{r}';\omega) \times \phi_{i'}(\mathbf{r}')\phi_{a'}^*(\mathbf{r}'). \quad (5)$$

The Hartree-exchange-correlation kernel $f_{\mathrm{HXC}}[n](\mathbf{r},\mathbf{r}';\omega)$ is the central quantity of linear-response TDDFT. In the time-domain, $f_{\mathrm{HXC}}[n](\mathbf{r}t,\mathbf{r}'t')$ is the functional derivative of the time-dependent Hartree-plus-exchange-correlation potential $v_H[n_t](\mathbf{r},t)+v_{\mathrm{XC}}[n_t](\mathbf{r},t)$ with respect to the time-dependent density $n_t(\mathbf{r}'t')$, evaluated at the ground-state density $n(\mathbf{r}')$ (see Sec. 4.3.2 of Ref. [40] for more details). Equations (4) and (5) are obtained from the linear response limit of the full TDDFT equations, in which N electrons evolve in the time-dependent KS potential

$$v_S[n_t](\mathbf{r},t) = v_{\mathrm{ext}}(\mathbf{r},t) + v_H[n_t](\mathbf{r},t) + v_{\mathrm{XC}}[n_t](\mathbf{r},t). \quad (6)$$

Here, $n_t = n(\mathbf{r},t)$ is the time-dependent density of the N KS electrons, which is the same as that of the interacting system [35].

To summarize, there are two stages. (1) The ground-state Kohn-Sham (KS) equations are solved to self-consistency; this requires an approximation to the ground-state exchange-correlation energy functional. Even if the (unknown) "exact" functional were used here, the excitations of the ground-state KS potential (i.e., differences between occupied and unoccupied KS orbital energies) could only be regarded as zeroth-order approximations to the true excitations of the system. (2) The KS frequencies are corrected via f_{HXC} to become the true excitations of the many-body system [36].

With rare exceptions, an adiabatic approximation (ATDDFT) is employed in this second step: the exchange-correlation potential at time t is approximated by that of a ground-state with the instantaneous density $n(\mathbf{r}t)$. This means that the Hartree-exchange-correlation kernel has no frequency-dependence in ATDDFT. An important consequence for the purposes of this paper is that states of double (or higher multiple) excitations cannot be captured within ATDDFT [41,42]; such excitations require a strongly frequency-dependent kernel. In the simplest (and common) adiabatic local-density approximation (ALDA), the approximation is local in space as well as time.

Notwithstanding the resounding success of TDDFT within existing approximations, different instances where the approximations fail have been identified. Charge-transfer excitations at long-range [43–45], conical intersections [46], states of multiple-excitation character [42,46], polarizabilities of long-chain polymers [47–49], Rydberg excitations [50,51], lie among the challenges in the linear response regime; nonsequential photoionization [30] and quantum control applications [52] are important challenges for approximations in the strong-field regime. Given the success of TDDFT for the vast majority of problems, and the fact that it scales in a reasonable way with system size while incorporating electron-correlation effects, there is a tremendous drive in the recent literature to understand and improve TDDFT approximations.

Elucidating the mechanism of interaction-induced chaos: type-KS vs type-f_{HXC} chaos. Consider now a system of N interacting electrons with Wigner-Dyson NNS statistics, and focus on the case where the external potential $v_{\mathrm{ext}}(\mathbf{r})$ is such that the classical dynamics of a single electron in $v_{\mathrm{ext}}(\mathbf{r})$ is integrable. The statistics of N noninteracting electrons moving in $v_{\mathrm{ext}}(\mathbf{r})$ follows that of the one-particle system, i.e., Poissonian in this integrable case. Suppose also that the exact functionals $E_{\mathrm{XC}}[n]$ and $f_{\mathrm{XC}}[n](\mathbf{r},\mathbf{r}';\omega)$ are known. The exact TDDFT procedure must transform the Poissonian noninteracting statistics to the correct interacting ones. In what follows, when the interacting system displays Wigner-Dyson statistics, we refer to this as the P→WD transition. Moreover, in studying how it does so, the mechanism for interaction-induced chaos can be better understood.

First, the ground-state KS potential $v_s(\mathbf{r})$ is found, and we ask: Is the classical dynamics of a single electron in $v_s(\mathbf{r})$ already chaotic? In this scenario, at least part of the interaction-induced chaos appears in DFT as a "chaotic kink" in the Hartree and/or exchange-correlation pieces of the potential. The "kink" is that piece of the KS potential due to which the single-particle classical dynamics is chaotic. Excitations from the bare KS potential will generally show in this case some degree of level repulsion, perhaps enough to agree with the experimental NNS distribution. We refer to this as type-KS chaos.

(We note here that it is preferable to perform the level statistics in such a way that N noninteracting electrons in a given potential follow the same type of distribution as a single electron in that potential: this can be achieved if the statistics are performed on energy levels of a fixed symmetry class. That is, if there are constants of the motion in addition to the total energy, one fixes the value of each of those constants. In the case of N noninteracting electrons, each orbital eigenvalue is a conserved quantity; therefore one fixes all except one, since the sum of the orbital energies gives the total energy. This amounts to considering only single excitations of the system; these can be out of any of the occupied orbitals, depending on which were chosen fixed but the resulting statistics will be independent of the choice).

In the second step of TDDFT, the bare KS excitations are corrected to the true ones using f_{HXC}: What is its effect on the statistics? Certainly if the KS system turned out to be integrable, then the entire job of transforming the statistics is done by the exact f_{HXC}. We refer to this as type-f_{HXC} chaos.

For N electrons in one dimension, type-KS chaos is impossible. The dynamics of a single electron in one dimension is obviously always integrable, since there is one conserved quantity (the energy of the electron) and one degree of freedom. Using the terminology above, the Kohn-Sham potential will never acquire a "chaotic kink" in one dimension. In more than one dimension the modulation of the external potential that is provided by the Hartree and xc terms [Eq. (3)] may induce chaotic motion on the one-electron dynamics. Nevertheless, as we will discuss in Sec. IV, type-f_{HXC} chaos

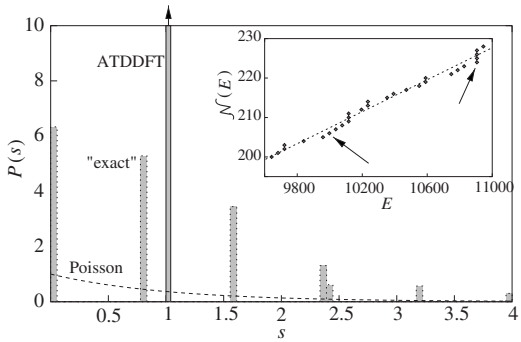

FIG. 1. Light-shaded bars: NNS histogram for the exact spectrum of two interacting electrons in a 1D box of length $L=1$ a.u. Dark-shaded bar: ATDDFT spectrum within exact exchange. Top arrow indicates that the bar keeps going up. Inset: small segment of staircase function $\mathcal{N}(E)$. The dotted line shows the smooth $\overline{\mathcal{N}}(E)$. Arrows point to the only two single excitations in this region.

is likely to be more common also in more than one dimension. Generally, most of the job required for the P→WD transition has to be done by f_{HXC}.

Of course in practice, approximate functionals must be used. The question then arises: what properties are needed in approximate kernels to achieve the correct statistics? Are the present-day approximations good enough to capture the P→WD transition as the interaction is turned on? In particular, the adiabatic approximation for the kernel: this mixes KS single excitations but cannot fold in multiple excitations [41,42]. This immediately raises a red flag as a chunk of the true excitations are excluded from consideration: how significant is this chunk? Even if the adiabatic kernel creates level repulsion by mixing singles only, if the double excitations compose a significant proportion of the spectra in a certain range, then the ATDDFT spectra would not be representative of the true system. The answers to these questions are likely system dependent. We illustrate in the next section most of the concepts discussed so far using a model of a one-dimensional quantum dot.

III. MODEL 1D QUANTUM DOT

Consider the problem of two electrons interacting via a soft-Coulomb potential $v_{ee}(x_1,x_2)=[1+(x_1-x_2)^2]^{-1/2}$ in a one-dimensional box of length L. A simple analysis shows that the matrix elements of v_{ee} scale approximately as $1/L$ (basis of noninteracting electrons), whereas the kinetic-energy matrix elements scale as $1/L^2$. The interaction in this sense becomes more important as the length of the box is increased. The noninteracting system is of course integrable, having two constants of the motion (the energies of the individual particles) for two degrees of freedom. The weakly interacting case (small L) is then almost integrable, and the strongly interacting case (large-L) nonintegrable. In fact, Ref. [24] shows clear signatures of interaction-induced chaos in a similar system. We start, however, in the weakly interacting limit, realized for $L=1$ a.u.

The light-shaded bars of Fig. 1 correspond to the nearest-neighbor-spacing (NNS) distribution $P(s)$ obtained via the following three steps. (1) Get the first $N_{\max}$ levels of the energy spectrum $\{E_i\}$ by exact diagonalization of the two-electron Hamiltonian, and discard the lowest $N_{\min}$. We typically used $N_{\max}=2000$, $N_{\min}=200$ and only states of even symmetry. (2) Unfold the staircase function $\mathcal{N}(E)$, representing the number of states having energy less than E, by applying the map $x_i=\overline{\mathcal{N}}(E_i)$, where $\overline{\mathcal{N}}$ is the smooth part of $\mathcal{N}$, found via a fourth-order polynomial fit to $\mathcal{N}(E)$. (3) Set $s_i=(x_{i+1}-x_i)$, and count $P(s)$, the number of occurrences for each $s_i/\bar{s}$, where $\bar{s}=\Sigma_i s_i/(N_{\max}-N_{\min})$. $P(s)$ then contains information about inherent fluctuations of the level spacings. As discussed in the introduction, these are generally Poissonian for integrable systems, and Wigner-Dyson-like for chaotic systems [53], but may also be nongeneric for some highly symmetric systems such as the one we are considering here. The exact histogram consists of a series of bars separated by gaps. The fluctuations around $\overline{\mathcal{N}}(E)$ (dotted line on the inset of Fig. 1) are evidently not random; they exhibit distinctive patterns, each of which gives rise to a different bar in the histogram. In the noninteracting limit, the problem of two particles with the same mass in a one-dimensional box is equivalent to that of a single particle in a two-dimensional square box, and the patterns just mentioned arise from the square symmetry of the problem. These remain in the weakly interacting regime. The histogram would be more Poissonian if the two particles had different masses, and even more so if the ratio of the two masses were an irrational number, as shown in Fig. 2 (and Ref. [54]).

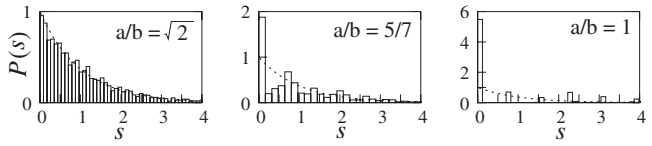

FIG. 2. The NNS distribution for a particle in a 2D rectangular billiard of sides a^2 and b^2 depends on the a/b ratio as indicated here. The dashed line corresponds to the Poisson distribution. (Shown first in Ref. [54].)

What does TDDFT predict for the histogram within the adiabatic approximation? A single bar centered at $s=1$ (dark-shaded bar in Fig. 1). We now explain why.

As discussed in Sec. II, the Kohn-Sham scheme transforms the original problem of two interacting electrons into that of a single electron moving in the potential $v_s(x)=v_{\mathrm{ext}}(x)+v_{\mathrm{HXC}}(x)$, where $v_{\mathrm{ext}}(x)$ is the external potential (box of unit length, in this case). Being a one-dimensional potential, it cannot exemplify type-KS chaos. The Hartree-exchange-correlation potential $v_{\mathrm{HXC}}(x)$ was found here within the exact-exchange approximation [55], as implemented in the octopus code [56]. $v_{\mathrm{HXC}}(x)$ is in this case simply a small bump at the bottom of the box (see solid line in lower panel of Fig. 3), having practically no influence on the high-energy spectrum of the noninteracting problem, except for a small shift in all the high-lying energies, irrelevant when the analysis of the differences between neighboring levels is made. The Kohn-Sham equations [Eq. (2)] yield a set of orbital energies $\{\varepsilon_i\}$, but only the subset of occupied orbitals is used to get the ground-state energy of the interacting system, as $E_0=\Sigma_{i\ \mathrm{occ}}\varepsilon_i+E_{\mathrm{HXC}}[n]-\int dx n(x)v_{\mathrm{HXC}}(x)$. The

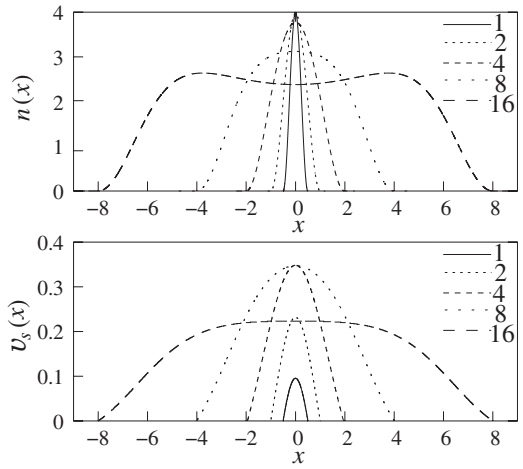

FIG. 3. Ground state density $n(x)$ and Kohn-Sham potential $v_s(x)$ for 2 interacting electrons in a 1D box, as its length is increased from $L=1$ to $L=16$. The walls of the boxes at $\pm L/2$ are not shown.

excited-state energies E_n^{TDDFT} are obtained within linear-response TDDFT as

$$E_n^{\mathrm{TDDFT}} = E_0 + \omega_n^{\mathrm{TDDFT}}, \tag{7}$$

where the squares of $\omega_n^{\mathrm{TDDFT}}$, $\Omega_n \equiv (\omega_n^{\mathrm{TDDFT}})^2$ are the eigenvalues of the matrix of Eq. (4).

The f_{HXC} kernel we employed is again that of exact-exchange, local in time [proportional to $\delta(t-t')$]. This level of approximation is sometimes called adiabatic time-dependent optimized effective potential, and is not the same as TDHF (see, for example, Ref. [57]). Since the kernel is local in time, its Fourier transform with respect to $t-t'$ is therefore frequency independent. As a consequence, from Eq. (4) and Refs. [41,42], ATDDFT only yields corrections to KS single excitations. Since the frequencies $\omega_n^{\mathrm{TDDFT}}$ of Eq. (7) are all mixtures of single excitations, the ATDDFT spectrum at this level contains no double excitations at all (or multiple excitations for $N>2$). This is a serious problem even at the low energies that are of interest for most quantum-chemical purposes, but in the present setting, the missing of double excitations is simply catastrophic. Single excitations are not more than a negligible fraction of the high-energy set of levels. The arrows of the inset in Fig. 1, for example, point to the only two single excitations found in the lowest-energy segment taken into account for our statistical analysis.

We are only one step away from concluding that in the energy range entering the statistical analysis, the ATDDFT staircase function is identical to the bare KS staircase function

$$\mathcal{N}^{\mathrm{ATDDFT}}(E) = \mathcal{N}^{\mathrm{KS}}(E). \tag{8}$$

To see this, we just point out that the expectation value of Eq. (5) becomes vanishingly small in the adiabatic approximation for high values of ω_q. It can be seen in Table I that for unoccupied orbital indices $a \gtrsim 10$, adiabatic single excitations barely differ from the KS ones on the scale of energy fluctuations.

TABLE I. Comparison of low-frequency excitations (in hartree) between bare Kohn-Sham energy differences $\varepsilon_a - \varepsilon_i$ and TDDFT frequencies obtained via Eq. (4) with the exact-exchange approximation to v_{XC} and an adiabatic approximation to f_{XC}.

$i \to a$	KS	TDDFT
$1 \to 2$	0.0939	0.2771
$1 \to 3$	0.3362	0.5132
$1 \to 4$	0.6736	0.8014
$1 \to 5$	1.1091	1.1963
$1 \to 6$	1.6425	1.7015
$1 \to 10$	1.7496	1.7628
$1 \to 20$	1.9319	1.9319

Furthermore, in the weakly interacting limit, $\mathcal{N}^{\mathrm{KS}}(E)$ coincides with the staircase function for a single electron in the presence of $v_{\mathrm{ext}}(x)$, since, as argued before, the effect of $v_{\mathrm{HXC}}(x)$ is negligible. $\mathcal{N}^{\mathrm{KS}}(E)$ has no fluctuations at all in this limit, being precisely proportional to $\sqrt{2E}$, and the unfolding process translates this into a histogram showing only $s=1$ spacings.

It may be argued that double excitations can simply be added to the ATDDFT spectrum by including the sums of $\varepsilon_a + \varepsilon_b$ with a and b running over all the unoccupied orbitals. This seems entirely sensible, and works of course in the non-interacting limit, but the adiabatic approximation yields no corrections to these states, and Eq. (8) still holds true.

We now discuss what occurs as we move toward the strongly interacting regime. Figure 4 shows the NNS histograms as the length of the box is increased from $L=10$ to $L=10^4$.

Strong level repulsion manifests itself with a marked decrease of small spacings. The histogram tends to a Wigner-Dyson distribution $P(s)=\frac{\pi}{2} s e^{-(\pi/4)s^2}$ for very wide boxes. This is a quantum signature of the underlying interaction-

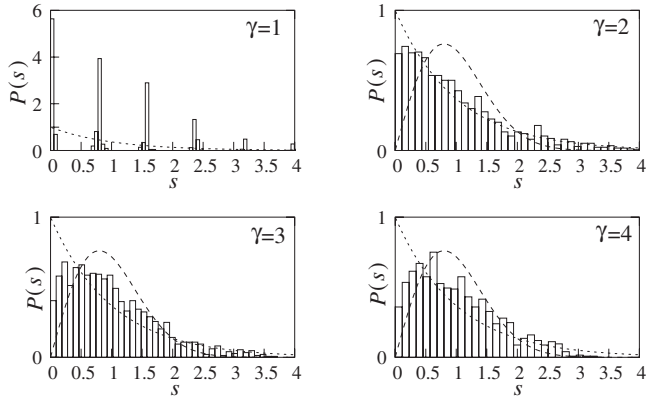

FIG. 4. NNS histograms for two interacting electrons in a 1D box of length $L=10^{\gamma}$. $P(s)$ approaches a Wigner-Dyson distribution (dashed) for very wide boxes, a signature of chaos in the underlying classical dynamics. The Poisson distribution is indicated by dotted lines.

induced chaos, as implied by the classical dynamics results obtained by Fendrik *et al.* [24], showing that apart from small regular regions in phase space, the dynamics of the system can become strongly chaotic due to electron-electron interactions. However, it follows from Eq. (8) that ATDDFT yields no level repulsion. Practically all levels entering the statistical analysis are double excitations. Even if we decided to artificially add these by summing unoccupied KS orbital energies, as discussed before, only a mixture of uncorrelated levels would result, i.e., a Poisson distribution $P(s)=e^{-s}$ with no level repulsion whatsoever (dotted lines in Fig. 4). This important signature of interaction-induced chaos is simply not captured by ATDDFT.

As the length of the box increases, localization of the electrons in opposite extremes of the box starts taking place, and convergence of the KS equations becomes problematic (we used the OCTOPUS code [56] for the DFT calculations). Figure 3 shows the evolution of the KS potential and ground-state density as L is increased from 1 to 16. The problems here are no different than those encountered when trying to describe the formation of a Wigner crystal [58] or other phenomena in the strongly correlated regime. There is already a hint of localization when $L=16$ (long-dashed line, upper panel of Fig. 3). The KS potential adopts the shape of a double well, with $v_{\mathrm{HXC}}(x)$ as the barrier in the middle, growing stronger with respect to level spacings as the length of the box increases.

IV. DISCUSSION AND OUTLOOK

Our example model system was an unfortunate one for the usual adiabatic approximations of TDDFT. The missing double excitations haunt the problem even in the integrable limit, making up the significant fraction of excitations in the true space and being crucial to bringing about the chaos. There is intensive development to go beyond the adiabatic approximation in TDDFT (e.g., Refs. [42,59–61]), and the progress has been successful in many cases. It will be interesting to adapt the kernel of Refs. [42,62]. to the case in the current paper.

We can now justify our claim of Sec. II that type-KS chaos is rare. Even in cases where $v_{\mathrm{HXC}}(\mathbf{r})$ develops a "chaotic kink" (see second part of Sec. II), level repulsion in the bare Kohn-Sham system will only be observed when the relevant excitations that enter the statistical analysis are of a single-particle nature. In such cases, ATDDFT should perform much better than in the model of Sec. III. The spectral properties of nonhydrogenic atoms in weak external electric or magnetic fields seem to be suitable examples. The joint effect of an ionic core of inner electrons (describable by a quantum defect for a series of single excitations) and the external field, has been shown to lead to chaos in some parameter regimes [16]. The fact that accurate quantum defects can be obtained from bare Kohn-Sham potentials, and that the external field appears explicitly in the KS equations, suggests that ATDDFT has a good chance to succeed in the description of this phenomenon. It will be interesting to compare the ATDDFT spectrum with that of the scatterer-perturber models in the literature, Refs. [16–19]. TDDFT treats all electrons quantum mechanically, and provides an *ab initio* method against which to compare the model potentials.

It should also be noted that the level-spacing statistics physically affect very high-temperature properties of the system. Other measures of chaos such as localization properties of wave functions are more relevant at usual lower temperatures. Before TDDFT can be used for these properties, one must first solve the TDDFT "observable problem," i.e., quantities that are directly given by the time-evolving density (or in perturbation theory, the density response), such as the excitation energies, oscillator strengths, or dipole moments, are simply extracted from the Kohn-Sham system. However, for properties that rely on other aspects of the interacting wave function, such as its localization in phase space, the information is not readily accessible from the Kohn-Sham system. Such cases demand the construction of appropriate functionals of the time-dependent density for the relevant wave function-dependent observable, often a challenging task (see, for example, Ref. [31]).

In summary, we have discussed prospects for using TDDFT to study how electron-interaction induces chaos in an otherwise integrable system. The scalability of TDDFT and its success in describing electron correlation in an ever-widening range of problems, make it attractive for this. Moreover, in principle, TDDFT should yield the correct level statistics for the interacting electronic system. We have discussed how the majority of currently-available approximate functionals, however, cannot capture the correct statistics in many cases of interest in quantum chaos, because of their inability to describe excited states of multiple-excitation character. Therefore challenges lie in developing approximate and easily implementable functionals for this purpose.

ACKNOWLEDGMENTS

We thank Jamal Sakhr for useful discussions. This work was supported in part by the National Science Foundation under Grant No. CHE-0310455. N.T.M. is grateful for financial support from the National Science Foundation CAREER program, Grant No. CHE-0547913.

[1] F. Haake, *Quantum Signatures of Chaos*, 2nd ed. (Springer, Berlin, 2000).

[2] O. Bohigas, M. J. Giannoni, and C. Schmit, Phys. Rev. Lett. **52**, 1 (1984).

[3] H. Wu, M. Vallières, D. H. Feng, and D. W. L. Sprung, Phys. Rev. A **42**, 1027 (1990).

[4] J. Zakrzewski, K. Dupret, and D. Delande, Phys. Rev. Lett. **74**, 522 (1995).

[5] O. Bohigas, in *Chaos and Quantum Physics*, edited by M. J. Giannoni, A. Voros, and J. Zinn-Justin, *Les Houches, Session LII* (Elsevier, Amsterdam, 1989).
[6] N. Bohr, Philos. Mag. **26**, 476 (1913).
[7] G. S. Ezra, K. Richter, G. Tanner, and D. Wintgen, J. Phys. B **24**, L413 (1991).
[8] G. Tanner, K. Richter, and J. M. Rost, Rev. Mod. Phys. **72**, 497 (2000).
[9] T. Guhr, A. Müller-Groeling, and H. A. Weidenmüller, Phys. Rep. **299**, 189 (1998).
[10] N. Rosenzweig and C. E. Porter, Phys. Rev. **120**, 1698 (1960).
[11] R. E. Trees, Phys. Rev. **123**, 1293 (1961).
[12] H. S. Camarda and P. D. Georgopulos, Phys. Rev. Lett. **50**, 492 (1983).
[13] V. V. Flambaum, A. A. Gribakina, G. F. Gribakin, and M. G. Kozlov, Phys. Rev. A **50**, 267 (1994).
[14] Th. Zimmermann, H. Köppel, L. S. Cederbaum, G. Persch, and W. Demtröder, Phys. Rev. Lett. **61**, 3 (1988).
[15] R. Püttner, B. Grémaud, D. Delande, M. Domke, M. Martins, A. S. Schlachter, and G. Kaindl, Phys. Rev. Lett. **86**, 3747 (2001).
[16] T. Jonckheere, B. Grémaud, and D. Delande, Phys. Rev. Lett. **81**, 2442 (1998).
[17] A. Matzkin and T. S. Monteiro, Phys. Rev. Lett. **87**, 143002 (2001).
[18] H. Held and W. Schweizer, Phys. Rev. Lett. **84**, 1160 (2000).
[19] K. Karremans, A. Kips, W. Vassen, and W. Hogervorst, Phys. Rev. A **60**, R2649 (1999).
[20] Ph. Jacquod and D. L. Shepelyansky, Phys. Rev. Lett. **79**, 1837 (1997).
[21] B. L. Altshuler, Y. Gefen, A. Kamenev, and L. S. Levitov, Phys. Rev. Lett. **78**, 2803 (1997).
[22] R. Berkovits and Y. Avishai, J. Phys.: Condens. Matter **8**, 389 (1996).
[23] M. Pascaud and G. Montambaux, Ann. Phys. **7**, 406 (1998).
[24] A. J. Fendrik, M. J. Sanchez, and P. I. Tamborenea, Phys. Rev. B **63**, 115313 (2001).
[25] L. E. F. Foa Torres, C. H. Lewenkopf, and H. M. Pastawski, Phys. Rev. Lett. **91**, 116801 (2003).
[26] Y. Alhassid, Rev. Mod. Phys. **72**, 895 (2000).
[27] K. Burke, J. Werschnik, and E. K. U. Gross, J. Chem. Phys. **123**, 062206 (2005).
[28] *Time-Dependent Density Functional Theory*, Lecture Notes in Physics, edited by M. A. L. Marques, C. A. Ullrich, F. Nogueira, A. Rubio, K. Burke, and E. K. U. Gross (Springer, Berlin, 2006).
[29] N. A. Nguyen and A. D. Bandrauk, Phys. Rev. A **73**, 032708 (2006).
[30] C. A. Ullrich and A. D. Bandrauk, in *Time-Dependent Density Functional Theory*, edited by M. A. L. Marques, C. A. Ullrich, F. Nogueira, A. Rubio, K. Burke, and E. K. U. Gross (Springer, Berlin, 2006), pp. 357–375.
[31] F. Wilken and D. Bauer, Phys. Rev. Lett. **97**, 203001 (2006).
[32] H. Jiang, D. Ullmo, W. Yang, and H. U. Baranger, Phys. Rev. B **69**, 235326 (2004).
[33] D. Ullmo, H. Jiang, W. Yang, and H. U. Baranger, Phys. Rev. B **71**, 201310(R) (2005).
[34] J. Lages and D. L. Shepelyansky, Phys. Rev. E **74**, 026208 (2006).
[35] E. Runge and E. K. U. Gross, Phys. Rev. Lett. **52**, 997 (1984).
[36] M. Petersilka, U. J. Gossmann, and E. K. U. Gross, Phys. Rev. Lett. **76**, 1212 (1996).
[37] M. E. Casida, in *Recent Developments and Applications in Density Functional Theory*, edited by J. M. Seminario (Elsevier, Amsterdam, 1996).
[38] W. Kohn and L. J. Sham, Phys. Rev. **140**, A1133 (1965).
[39] E. Prodan and W. Kohn, Proc. Natl. Acad. Sci. U.S.A. **102**, 11635 (2005).
[40] M. A. L. Marques and K. U. Gross, in *A Primer in Density Functional Theory*, edited by C. Fiolhais, F. Nogueira, and M. Marques (Springer-Verlag, New York, 2003).
[41] D. J. Tozer and N. C. Handy, Phys. Chem. Chem. Phys. **2**, 2117 (2000).
[42] N. T. Maitra, F. Zhang, R. J. Cave, and K. Burke, J. Chem. Phys. **120**, 5932 (2004).
[43] A. Dreuw, J. Weisman, and M. Head-Gordon, J. Chem. Phys. **119**, 2943 (2003).
[44] D. Tozer, J. Chem. Phys. **119**, 12697 (2003).
[45] N. T. Maitra and D. Tempel, J. Chem. Phys. **125**, 184111 (2006).
[46] B. G. Levine, C. Ko, J. Quenneville, and T. J. Martinez, Mol. Phys. **104**, 1039 (2006).
[47] S. J. A. van Gisbergen, P. R. T. Schipper, O. V. Gritsenko, E. J. Baerends, J. G. Snijders, B. Champagne, and B. Kirtman, Phys. Rev. Lett. **83**, 694 (1999).
[48] M. van Faassen, P. L. de Boeij, R. van Leeuwen, J. A. Berger, and J. G. Snijders, Phys. Rev. Lett. **88**, 186401 (2002).
[49] P. Mori-Sánchez, Q. Wu, and W. Yang, J. Chem. Phys. **119**, 11001 (2003).
[50] A. Wasserman and K. Burke, Phys. Rev. Lett. **95**, 163006 (2005).
[51] C. P. Hu and O. Sugino, J. Chem. Phys. **126**, 074112 (2007).
[52] I. Serban, J. Werschnik, and E. K. U. Gross, Phys. Rev. A **71**, 053810 (2005).
[53] T. A. Brody, J. Flores, J. B. French, P. A. Mello, A. Pandey, and S. S. M. Wong, Rev. Mod. Phys. **53**, 385 (1981).
[54] M. V. Berry and M. Tabor, Proc. R. Soc. London, Ser. A **356**, 375 (1977).
[55] J. B. Krieger, Y. Li, and G. J. Iafrate, Phys. Rev. A **45**, 101 (1992).
[56] http://www.tddft.org/programs/octopus; M. A. L. Marques, A. Castro, G. F. Bertsch, and A. Rubio, Comput. Phys. Commun. **151**, 60 (2003).
[57] Y. Shigeta, K. Hirao, and S. Hirata, Phys. Rev. A **73**, 010502(R) (2006).
[58] H. B. Shore, E. Zaremba, J. H. Rose, and L. Sander, Phys. Rev. B **18**, 6506 (1978).
[59] G. Vignale and W. Kohn, Phys. Rev. Lett. **77**, 2037 (1996).
[60] I. V. Tokatly, Phys. Rev. B **71**, 165104 (2005); I. V. Tokatly, *ibid.* **71** 165105 (2005).
[61] Y. Kurzweil and R. Baer, Phys. Rev. B **72**, 035106 (2005); Y. Kurzweil and R. Baer, J. Chem. Phys. **121**, 8731 (2004).
[62] R. J. Cave, F. Zhang, N. T. Maitra, and K. Burke, Chem. Phys. Lett. **389**, 39 (2004).